Proceedings

Advanced Materials for Construction of Bridges, Buildings, and Other Structures III

Engineering Conferences International *Year* 2003

Interface Behaviour in FRP Plates Bonded to Concrete: Experimental Tests and Theoretical Analyses

Ciro Faella * Enzo Martinelli†
Emidio Nigro‡

*University of Salerno, c.faella@unisa.it
†University of Salerno, e.martinelli@unisa.it
‡University of Naples “Federico II”, emidio.nigro@unina.it

INTERFACE BEHAVIOUR IN FRP PLATES BONDED TO CONCRETE: EXPERIMENTAL TESTS AND THEORETICAL ANALYSES

Ciro Faella , Full Professor, DICiv, University of Salerno (Italy)
Via Ponte don Melillo, 84084, Fisciano (SA) - Italy
T: 39-89-964043; F: 39-89-964045; E: c.faella@unisa.it
Enzo Martinelli, Post-Doctoral Fellow, DICiv, University of Salerno (Italy)
T: 39-89-964098; F: 39-89-964045; E: e.martinelli@unisa.it
Emidio Nigro, Associate Professor, DAPS, University of Naples “Federico II” (Italy)
Via Claudio, 80125, Napoli - Italy
T: 39-81-7683491; E: emidio.nigro@unina.it

ABSTRACT

Simplified models for simulating FRP-to-concrete interface behavior are introduced and empirical relationships are utilized for their calibration. Moreover, the results of pull-out tests on FRP-to-concrete joints are presented. They are utilized in calibrating a bilinear shear-stress-to-interface-slip relationship by means of an inverse identification procedure.

INTRODUCTION

Peeling phenomena resulting in premature failures are quite frequent in R.C. beams strengthened with FRP sheets. Several scientific contributions have been proposed by various researchers in the last ten years concerning both with the interface stress evaluation and adhesive-concrete bond interface behavior.
Chen and Teng (1) reported an overview of some models for evaluating the ultimate strength of FRP or Steel plates epoxy-bonded to concrete. They have been classified into three categories: empirical models, based directly on the regression of experimental data, fracture mechanics, based models design proposals that generally make use of some simplified assumptions. In particular, the models belonging to the second category consist in introducing various expressions for fracture energy, representing relationships between interface slip and tangential stress.
Neubauer and Rostasy (2) starting from previous researches assumed a bi-linear relationship between slip and interface shear stress, simulating a first range of elastic behavior, followed by a second and larger one accounting for the softening behavior of concrete beneath the epoxy resin. In fact, concrete cracking due to high interface shear stress results in softening behavior of the epoxy-concrete interface as a whole (bi-linear relationship “a” in Fig. 1). Due to the greater importance of the softening range with respect to the elastic one for evaluating the ultimate strength of the FRP-to-concrete joint, a linear descending simplified relationship may be assumed (descending relationship “b” in Fig. 1). Bi-linear relationship has been chosen by Wu and Yin (3) to model the fracturing behavior of FRP-strengthened concrete structures: they studied the mode II crack (shear mode) occurring in the adhesive layer and proposed a smeared crack model for simulate the microcracking phenomena occurring at the adhesive-

concrete interface, resulting in a progressive loss of strength of the epoxy FRP-to-concrete joint as a whole.

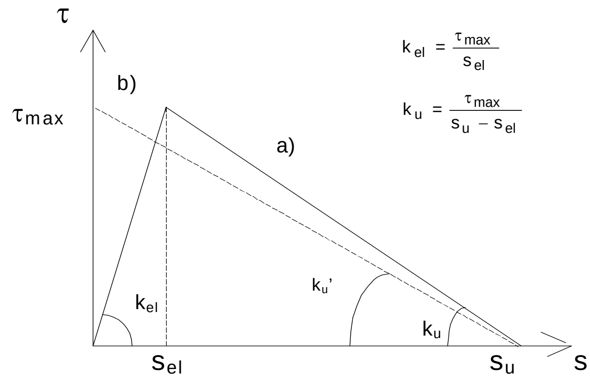

Fig. 1: Two possible τ-s relationships: a) bi-linear; b) linear softening.

Several efforts have been carried out by various researchers about either evaluating stress concentration in the adhesive interface and estimating its strength.
Under the experimental standpoint, various testing techniques have been proposed for investigating the interface behavior. Jones et al. (4) tested scaled beams strengthened with steel plates characterized by different dimensions and arrangements of plates; Bizindavy (5) carried out similar experiments on beams strengthened by FRP sheets: both observed premature beam failures due to interface debonding of the strengthening plates. Instead of testing strengthened beams as a whole, Bizindavy (5) and Chajes et al. (6) performed pull-out tests on FRP-to-concrete epoxy joints in order to evaluate the interface behavior by reproducing the situation of the cut-off section in strengthened beams where stress concentrations arise. However, largely scattered results have been obtained for bond strength due to different testing methods adopted by the various researchers. Horigucki and Saeki (7) just focused on the effect of testing methods by comparing the results in terms of (average) bond strength obtained with three types of tests; they found that tensile tests provide always the higher bond strength while shear pull-out tests give generally the lower values. It is easy to understand that such a general trend is mainly due to the stress distribution induced by the two above mentioned tests: in particular, tensile tests results in uniform tensile stress at the interface while shear tests induce a normal and shear stress concentrations close to the pulling out force application point, as it will be widely shown in the following.
Under the theoretical point of view various one-dimensional models have been carried out for estimating stress concentrations in the adhesive layer. Roberts (8) proposed one of the first formulation for evaluating normal and shear stress in the adhesive layer by means of a simple uncoupled approach. In the following years other proposals have been carried out among which the ones by Saadatmanesh et al (9) and Täljsten (10), both providing a closed form solution for shear and normal stress concentrations. Moreover, Brosens and van Gemert (11) proposed a Mohr-Coulomb-like failure criterion for evaluating limit combinations of shear and normal stresses in the adhesive-concrete interface.
Both experimental findings and theoretical models have been utilized to carry out debonding strength models for FRP-strengthened RC beams: Smith and Teng (12) examined twelve different approaches available in the scientific literature for assessing their strengths and weaknesses. They demonstrated the great scatter characterizing such models and proposed another one providing a shear force limitation at the cut off section.
The present paper, starting from the above mentioned studies, deals with the comparison of some proposals about FRP-to-concrete interface behavior under both service and ultimate loads. European (Fib bulletin 14, (13)) code of standards about r.c beams strengthened by FRP

sheets will be examined in order to compare their provisions in evaluating adhesive-concrete interface strength.
In the last sections of the present work, the results of an experimental program of pull-out tests on FRP-to-concrete joints carried out at the Laboratory of Structures of the University of Salerno and fully reported in Faella et al. (14) are presented. On the basis of the experimental results an indirect identification procedure is then carried out for calibrating the bilinear ascending-softening relationship chosen for characterizing the joint behavior. In fact, neither bond strength nor stiffness can be determined by means of a direct evaluation: for this reason measured strain values will be utilized to identify the interface relationship.

THEORETICAL MODELS AND CODE PROVISIONS

The present section deals with comparing some simplified models for interface behavior of FRP-to-Concrete epoxy joints. Some code provisions derived by this kind of models will be considered.

Interface behavior

The simplest way for simulating FRP-to-concrete interface behavior consists in assuming uncoupled models for shear and normal stresses (Fig. 2).

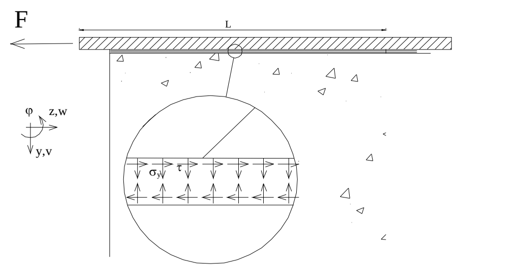

Fig. 2: FRP-to-concrete joint.

Equilibrium and compatibility conditions in z-direction stated as follows

$$\frac{d\sigma_z}{dz} + \frac{\tau(s)}{t_p} = 0 \qquad\qquad \varepsilon = \frac{ds}{dz} \;, \tag{1}$$

lead to the following differential equation in terms of shear stress $\tau(s)$ and interface slip s:

$$\frac{d^2 s}{dz^2} + \frac{\tau(s)}{E_p t_p} = 0 \;, \tag{2}$$

where E_p is the plate Young modulus and t_p is its thickness. Assuming the bi-linear relationship for $\tau(s)$ represented in Fig. 1 two cases can occur. If $s \le s_{el}$ throughout all the bonded length (elastic behaviour) the following exponential solution can be derived (Fig. 3a):

$$\tau = \alpha_{el} \frac{P}{b_p} \frac{\cosh[\alpha_{el}(L-z)]}{\sinh(\alpha_{el} L)} \qquad\qquad s = \frac{\tau}{k_{el}} = \frac{\alpha_{el}}{k_{el}} \frac{P}{b_p} \frac{\cosh[\alpha_{el}(L-z)]}{\sinh(\alpha_{el} L)} \;, \tag{3}$$

being

$$\alpha_{el} = \sqrt{\frac{k_{el}}{E_p t_p}} \;. \tag{4}$$

The maximum “elastic” interface slip is attained for a force P_{el}:

$$P_{el} = \frac{\tau_{max}}{\alpha_{el}} \cdot b_p \cdot \tanh(\alpha_{el} L) \ . \qquad (5)$$

Whenever P overcomes P_{el}, slip in the bond length are greater than s_{el} between the application point of the pulling out force and the abscissa z_{el}, where $s = s_{el}$ (curve b in Fig. 3).

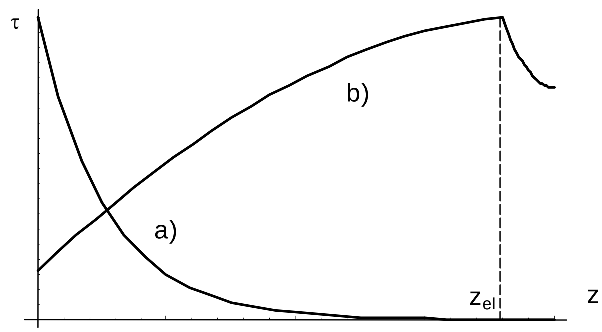

Fig. 3: Interface shear stress: a) at the elastic limit, b) beyond the elastic limit.

In this case, two different expressions can be obtained for the two regions of the bonding length:

$$\tau = \begin{cases} \tau_{max} \left\{ \cosh\left[\alpha_u (z - z_{el})\right] + \sqrt{\dfrac{k_{el}}{k_u}} \sinh\left[\alpha_u (z - z_{el})\right] \cdot \tanh\left[\alpha_{el} (L - z_{el})\right] \right\} & \text{in} \quad z \le z_{el} \\ \tau_{max} \dfrac{\cosh\left[\alpha_{el} (L - z)\right]}{\cosh\left[\alpha_{el} (L - z_{el})\right]} & \text{in} \quad z > z_{el} \end{cases} \qquad (6)$$

being:

$$\alpha_u = \sqrt{\frac{\tau_{max} / (s_u - s_{el})}{E_p t_p}} = \sqrt{\frac{k_u}{E_p t_p}} \ . \qquad (7)$$

The values of the force P (greater than P_{el}) corresponding to the given position of the transition point z_{el} can be obtained by integrating shear stresses along the bonding length. The maximum value P_{max} may be searched by varying the position of z_{el} between 0 and L.

Serviceability Limit State

Verification of bond interface microcracking is one of the characteristic aspects of the Serviceability Limit State for reinforced concrete beams strengthened by externally bonded FRP plates. Fib bulletin 14 (13) requires an explicit check of the peak value reached by shear stress close to the cut-off section of the plate. It assumes the formula proposed by Roberts (8) for evaluating the maximum shear stress by summing the shear stress obtained according to the Jourawsky Theory and an additional one due to the abrupt change in the cut-off section, obtained by analogy with the first relationship (3) where the force P is evaluated depending on the bending moment and the section lever arm: the latter one is generally predominant. For this reason, estimating such a peak value depends strongly on the parameter α_{el} related to the ratio between the adhesive shear stiffness k_{el} and the plate axial stiffness $E_p t_p$. The latter term is generally easy to evaluate; on the contrary estimating the former one is not so straightforward due to the following reason. Usually, theoretical models assumed that concrete layer beneath the adhesive does not strain; under this hypothesis strain concentration develops in the epoxy layer. Such a behavior is likely to occur only if adhesive is much more flexible than concrete. On the contrary, participation in shear strain of the concrete layer beneath the adhesive is as great as the resin-to-concrete flexibility ratio increases. A one-dimensional model assumed for simulating the FRP-to-concrete joint needs to take into account the possible participation in shear strain of the concrete beneath the adhesive layer. In fact, epoxy resin and concrete can be thought like two springs in series (Fig. 4a) whose effective flexibility can be evaluated by summing the flexibility of each one. The effective stiffness $k_{el,eff}$ or, even, the equivalent epoxy thickness $t_{a,eff} = k_{el,eff} / G_a$ depends on the adhesive-to-concrete stiffness ratio. Fig. 4b shows the correlation between $t_{a,eff}$ and the $G_a / (G_c t_a)$ ratio for a FRP-to-concrete joint (like the one represented in Fig. 2), by minimizing the scatter between the axial strain patterns obtained by means of a 2D-FEM analysis and the one-dimensional model consisting in equations (1) and (3).

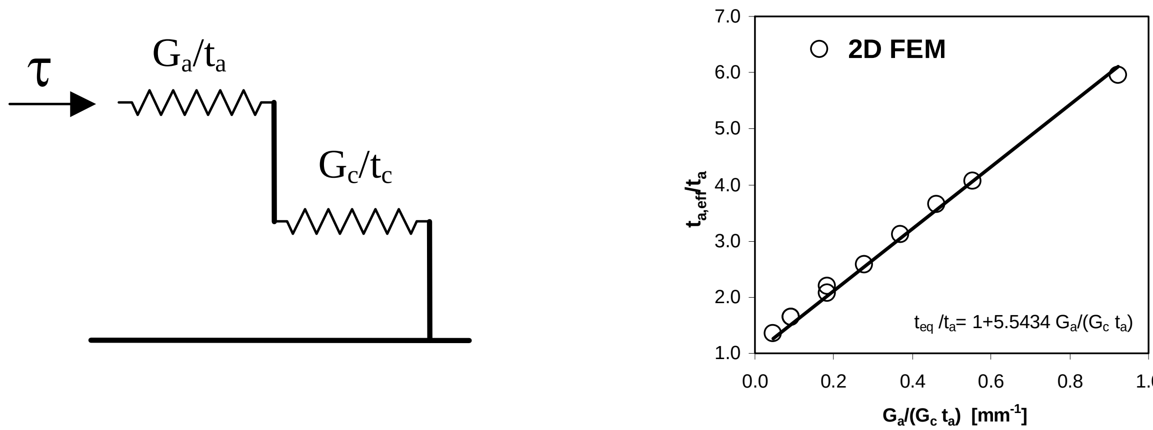

a) spring in series; b) equivalent epoxy thickness

Fig. 4: Effect of concrete flexibility on the effective thickness of the epoxy resin layer

Further investigations, both experimental and analytical, have to be carried out to quantify the influence of the above mentioned phenomenon on the stress distribution represented in Fig. 3. In fact, the verification of bond interface cracking is less penalizing at the Serviceability Limit State if the effective value of the adhesive layer increases (and, even, the effective adhesive stiffness decreases).

Ultimate Limit State

Bi-linear ascending-softening relationship for describing the interface behavior can by roughly simplified by considering a rigid-softening relationship (Fig. 1b) and assuming $k_u' \approx k_u$. Under this hypothesis the ultimate capacity of the FRP-to-concrete joint can be evaluated as follows:

$$P_{max} = \tau_{max} \cdot L \cdot b_p \cdot \frac{\sin(\alpha_u L)}{\alpha_u L} \quad \text{with} \quad L \le L_{eff} = \frac{\pi}{2\alpha_u} . \tag{8}$$

The inequality in equation (8) means that s in not greater than s_u throughout all the bonding length L of the FRP-to-Concrete joint. When L reaches L_{eff}, s overcomes s_u in the portion of the joint close to the force P; for this reason, no further increase can be obtained for L greater than L_{eff} and the maximum ultimate capacity $P_{max,Leff}$ can be expressed as follows:

$$P_{max,Leff} = \tau_{max} \cdot \sqrt{\frac{E_p t_p}{k_u}} \cdot b_p \quad \text{or} \quad P_{max,Leff} = \sqrt{2 G_f E_p t_p} \cdot b_p . \tag{9}$$

being G_f the fracture energy of the joint, namely, the area under the straight line b in Fig. 1.

Fib bulletin 14 (13), (in the section devoted to the "ULS verification of peeling-off at the end anchorage and at flexural cracks") introduces various formulae obtained by different authors in a generally empirical way on the basis of experimental data. By comparing the above theoretical formulae with respect to the corresponding experimental ones provided by the Fib bulletin, a calibration of the parameters defining the simplified softening $\tau - s$ relationship can be obtained and reported as follows:

$$L_{eff} = \sqrt{\frac{E_p t_p}{2 \cdot f_{ctm}}} \quad [\mathrm{mm}] \qquad \Rightarrow \qquad k_u = \frac{\pi^2}{2} f_{ctm} \quad [\mathrm{N/mm^3}]\,, \tag{10}$$

$$\begin{aligned} P_{max,Leff} &= \alpha \cdot c_1 \cdot k_c \cdot k_b \sqrt{E_p t_p f_{ctm}} \cdot b_p = \\ &= 0.50 \div 0.76 \sqrt{E_p t_p f_{ctm}} \cdot b_p \end{aligned} \quad \Rightarrow \quad \begin{aligned} G_f &= 0.24 \div 0.29 \cdot f_{ctm} \quad [\mathrm{N/mm}] \\ \tau_{max} &= 1.11 \div 1.69 \cdot f_{ctm} \quad [\mathrm{N/mm^2}] \end{aligned}\,. \tag{11}$$

Further attempts for estimating the main parameters of the interface $\tau - s$ relationship will be carried out and shown in the following on the basis of some experimental data.

EXPERIMENTAL TESTS

FRP-to-concrete joint behavior has been observed by means of twenty single-lap pull-out tests carried out at the Laboratory of Structures of the University of Salerno; a complete report of such tests has been proposed by Faella et al. (14) and tests set-up is represented in Fig. 5a. Test specimens consist in FRP laminate bonded to concrete blocks by means of an epoxy-resin layer. Five different bonding lengths ranging between 50 and 250 mm have been considered in order to point out the influence of such a parameter on the joint behavior. Pull-out tests have been conducted in displacement control.

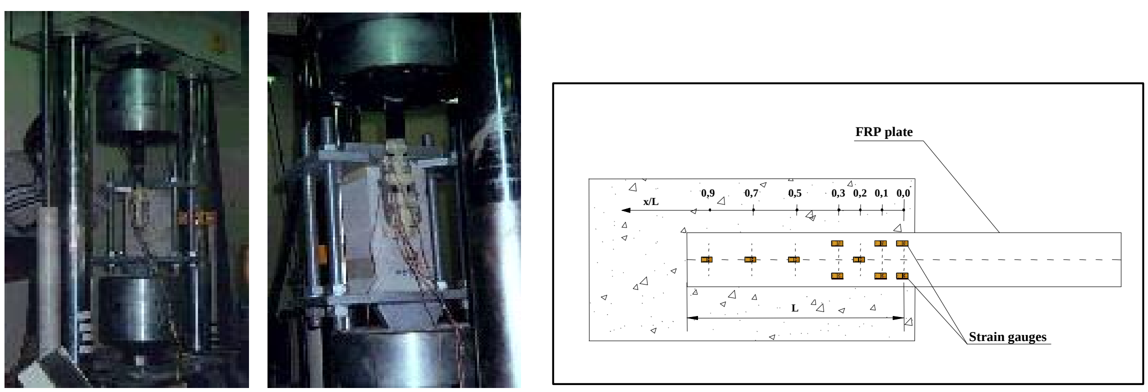

a) test device and specimens b) typical strain gauge arrangement

Fig. 5: Pull-out tests and related instrumentation

All specimens have been instrumented with a series of strain gauges (Fig. 5b) for measuring the strain pattern at each load level resulting for the imposed displacement.

Axial strains have been measured along the FRP bonded length and reported in the following section. Average values of shear stress $\bar{\tau}_i$ between two adjacent strain gauges measuring strains ε_{i+1} and ε_i can be obtained by means of the following equilibrium condition:

$$\bar{\tau}_i = \frac{(\varepsilon_{i+1} - \varepsilon_i)}{\Delta z_i} \cdot E_p t_p\,. \tag{12}$$

Finally, it is useful to notice that specimens generally fail in the two following ways:

- peeling failure, by removing a thin (about 1 mm) concrete layer beneath the adhesive;
- ripping failure, by removing a thick (about 1-2 cm) concrete layer.

DATA ELABORATION

In this section an indirect identification of the interface relationship between shear stress and interface slip will be carried out making use of the experimental data in terms of axial strains along the bond length.

A general function $\varepsilon_c(z; k_{el}, \tau_{max}, k_u)$, depending on a given $\tau - s$ relationship defined by three parameters (for example, k_{el}, τ_{max}, k_u in Fig. 1) can be introduced for calculating the strain value at the abscissa z due to a pulling-out force P. The values obtained by means of such a function in correspondence of the points z_j where experimental data have been measured, can utilized for evaluating a scatter function Δ defined as follows:

$$\Delta(k_{el}, \tau_{max}, k_u) = \sum_{i=1}^{n_{liv}} \sum_{j=1}^{n_{mis}} \left[\varepsilon_{m,j}^{(i)} - \varepsilon_c^{(i)}(z_j; k_{el}, \tau_{max}, k_u)\right]^2 , \qquad (13)$$

by comparing the values $\varepsilon_{m,j}^{(i)}$ measured at the j-th strain gauge for the i-th load value. The scatter function $\Delta = \Delta(k_{el}, \tau_{max}, k_u)$ has to be minimized considering the range of variation of the three parameters on which it depends and the following constraint condition:

$$P_{max}(k_{el}, \tau_{max}, k_u, L) = P_{max,m} , \qquad (14)$$

stating that the assumed $\tau - s$ relationship gives an ultimate capacity $P_{max}(k_{el}, \tau_{max}, k_u, L)$ equal to the measured value $P_{max,m}$ for an FRP-to-concrete joint whose bonding length is equal to L.

In such a manner the indirect identification of the joint $\tau - s$ relationship is represented by a constrained optimization problem.

The minimization procedure is performed in two steps for the sake of simplicity and efficiency. The first one deals only with the elastic parameter k_{el} and is based on the lower load level (lesser than 1/10 of the maximum joint capacity): the optimal value $\bar{k}_{el}$ of the slip modulus k_{el} is obtained by the following condition:

$$\bar{k}_{el} = \arg\min \Delta(k_{el}) . \qquad (15)$$

The second step deals with the other two parameters that can be obtained by solving the following restrained minimum problem:

$$\{\bar{\tau}_{max}, \bar{k}_u\} = \arg\min \Delta(\bar{k}_{el}, \tau_{max}, k_u) \qquad \text{with} \qquad P_{max}(\bar{k}_{el}, \bar{\tau}_{max}, \bar{k}_u, L) = P_{max,m} . \qquad (16)$$

The indirect identification procedure outlined above has been carried out for all the experimental results obtained in the campaign described in the previous section. In the following a comparison between the experimental results and the analytical values obtained by means of equation (6) assuming the identified $\tau - s$ relationship is reported in Fig. 6 - Fig. 8.

The above mentioned figures show that the indirect identification procedure leads to a very good agreement with the experimentally observed behavior. The following Fig. 9 represents the correlation between some parameters defining the identified $\tau - s$ relationship and the average cube strength f_{cm} obtained by compression testing of the various specimens.

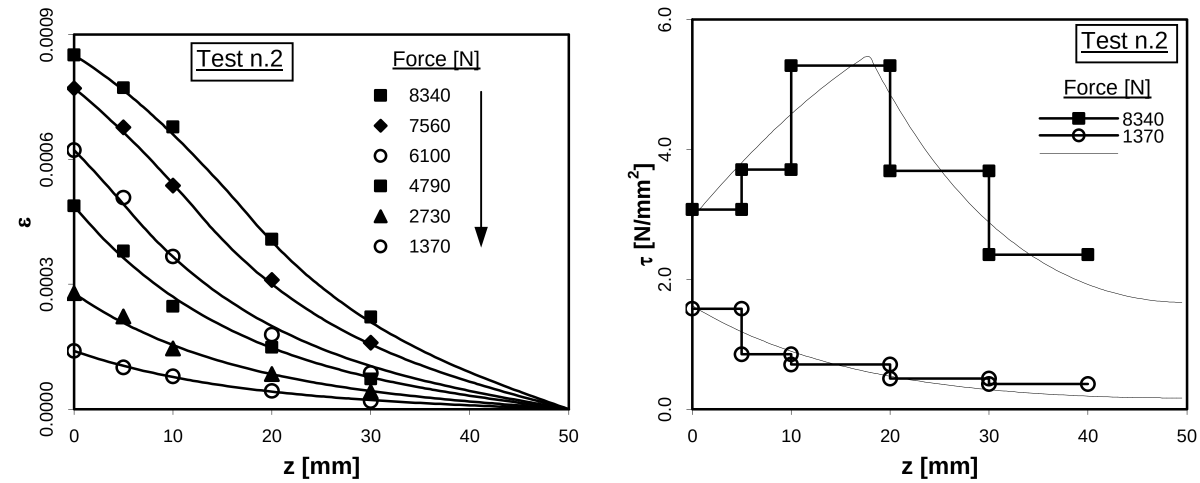

Fig. 6: Experimental results and analytical simulation for specimen 2 (L=50 mm).

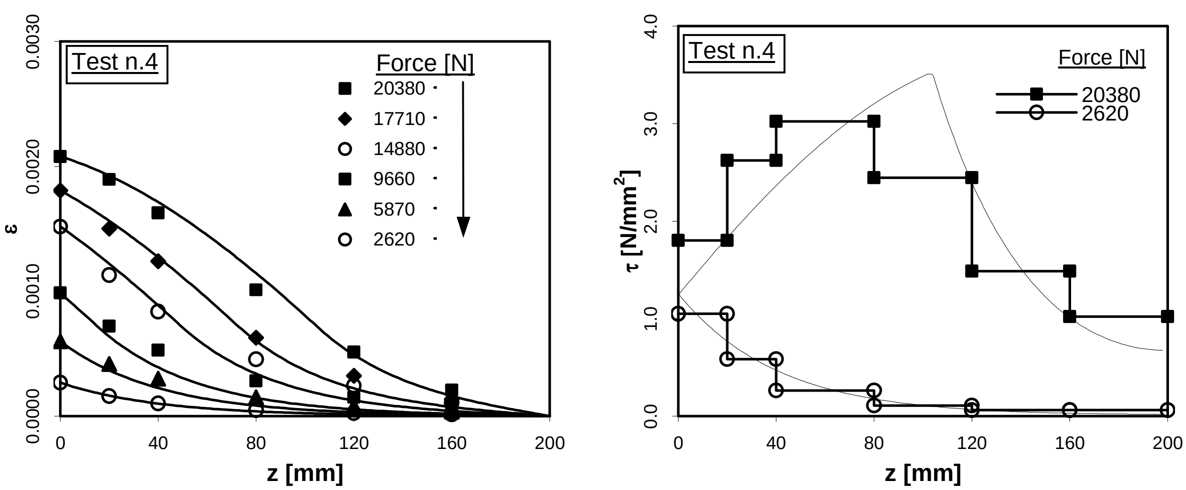

Fig. 7: Experimental results and analytical simulation for specimen 4 (L=200 mm).

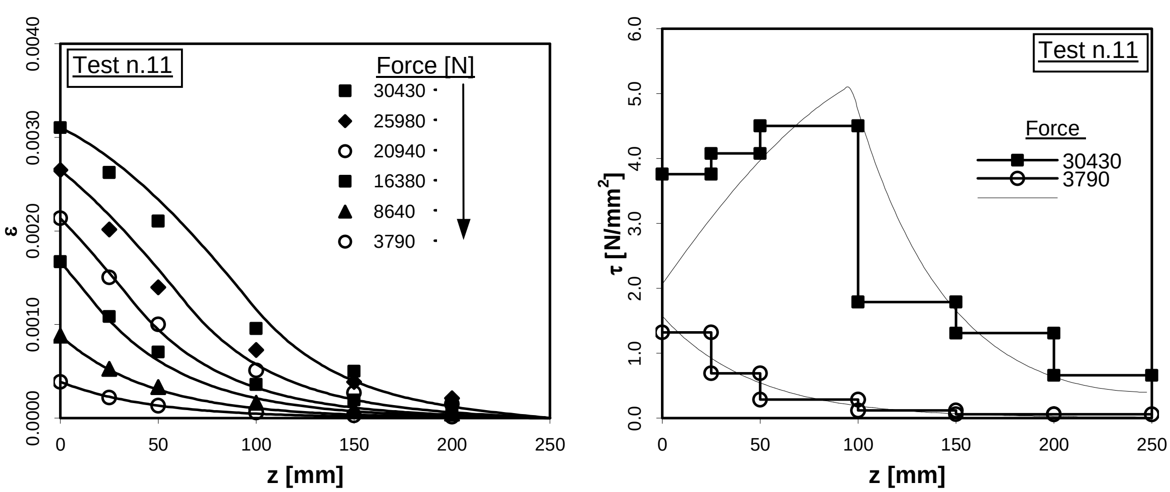

Fig. 8: Experimental results and analytical simulation for specimen 4 (L=250 mm).

In particular, Fig. 9a shows such a correlation in terms of maximum shear stress τ_{max} while Fig.

9b focuses on the ultimate slip value s_u: numerical interpolation confirms the expected trends (τ_{max} increases and s_u decreases as the concrete cylindrical strength increases) even if both figures show weak correlation mainly due to experimental uncertainties.

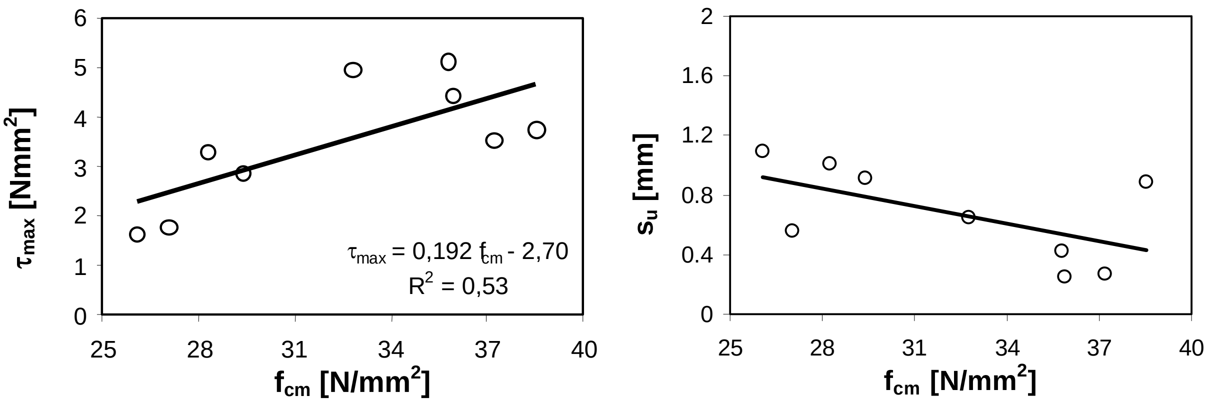

a) maximum shear stress τ_{max} b) ultimate slip s_u

Fig. 9: Correlation between the identified relationships parameters and concrete strength.

Finally, the same maximum stress values can be compared with the various empirical formulae due to different researchers and provided by the Fib Bulletin 14 (13) (ULS verification – Approaches 1, 2 and 3): Fig. 10 confirms the great variability of the considered quantity.

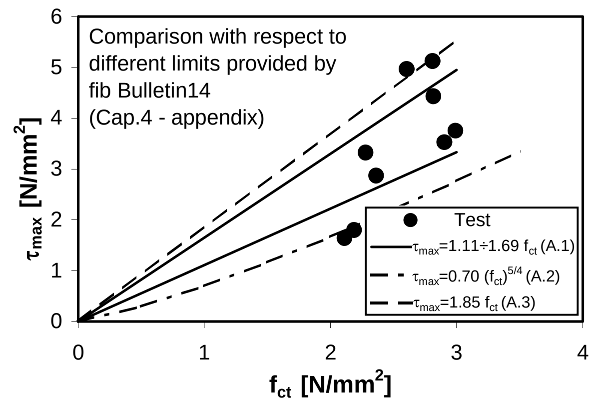

Fig. 10: Comparison with respect to some formulae proposed by the fib – bulletin 14 (4).

CONCLUSIONS

In the present paper some theoretical models simulating the behavior of FRP-to-concrete interface of reinforced concrete beams strengthened by FRP bonding have been considered. In particular, the bi-linear ascending-softening relationship proposed by various authors for describing the fracturing behavior of the adhesive interface has been utilized for obtaining a closed form relationship of the shear stress along the bonding length of an FRP-to-concrete joint. Such a relationship has been assumed for reproducing the stress transfer phenomena developing in correspondence of the FRP cut-off section. These closed form formulae can be utilized either for simulating the shear stress and strain patterns under service loads (elastic range) and ultimate loads (post-elastic softening range).

Some code provisions about both Serviceability and Ultimate Limit State have been briefly outlined and utilized to have a first possible calibration of the parameters characterizing the adhesive-to-concrete interface behavior involved in the above mentioned formulae .

Finally a series of suitably instrumented experimental tests have been presented and utilized to obtain the interface relationship in terms of $\tau - s$ curve by means of an indirect identification procedure. Even if such a procedure needs other improvements, it represents the straightest way for obtaining the whole bonding relationship for FRP-to-concrete interface on which rational methods for Ultimate and Serviceability verifications can be based.

REFERENCE

(1) J.F. Chen, J.G. Teng**:** "Anchorage Strength Models for FRP and Plates Bonded to Concrete", ASCE Journal of Structural Engineering, vol. 127, No. 7, July, 2001, 784-791;

(2) U. Neubauer, F.S. Rostasy**,** "Bond Behaviour of CFRP-Laminates for the Strengthening of Concrete Members", Proceedings of Composite Construction – Conventional and Innovative, Innsbuck (Austria), 16-18 September 1997, 717-724;

(3) Z. Wu, J. Yin: "Fracturing behaviors of FRP-strengthened concrete structures", Engineering Fracture Mechanics, vol. 70, 2003, 1339-1355;

(4) R. Jones, R. N. Swamy, A. Charif: "Plate separation and anchorage of reinforced concrete beams strengthened by epoxy-bonded steel plates", The Structural Engineer, Vol. 66, No. 5, March 1988, 85-94;

(5) L. Bizindavyi. "Étude expérimentale et analytique du comportement de l'interface entre les structures en béton armé et les plaques de renfort externe en polymères renforcés de fibres". *Ph.D. Thesis,* Université de Sherbrooke, 1999.

(6) Chajes, M.J., Finch, W.W., Januszka, T.F., and Thomson, T.A. (1996). "Bond and Force Transfer of Composite-Material Plates Adhered to Concrete," *Structural Journal*, ACI, 93(2), 208-217;

(7) T. Horigucki, N. Saeki**,** "Effect of Test Methods and Quality of Concrete on Bond Strength of CFRP Sheet", Proceedings of the 3rd International Symposium on Non-Metallic (FRP) Reinforcement for Concrete Structures, Sapporo (Japan), October 1997, vol. 1, 265-270, 265-270;

(8) T. M. Roberts: "Approximate analysis of shear and normal stress concentrations in the adhesive layer of plated RC beams", The Structural Engineer, Vol. 66, No. 5, March 1988, 85-94;

(9) Malek A. M., Saadatmanesh H., Ehsani M. R., Prediction of failure load of R/C beams strenghtened with FRP plate due to stress concentration at the plate end, ACI Structural Journal, Vol. 95, No. 2, March-April 1998, 142-152;

(10) B. Täljsten: Strengthening of Beam by Plate Bonding , ACSE Journal of Materials in Civil Engineering, vol. 9, No. 4, November 1997, 206-212;

(11) K. Brosens, D. Van Gemert: Anchorage of externally bonded reinforcements subjected to combined shear/bending action, CICE2001, International conference on FRP composites in Civil Engineering, 12 - 14 December 2001, Hong Kong;

(12) S. T. Smith, J.G. Teng: FRP-strengthened RC beams. II: assessment of debonding strength models, Engineering Structures, 24, 2002, 397-427;

(13) FiB: Bulletin d'information n. 14: **"**Externally bonded FRP reinforcement for RC structures", July 2001;

(14) C. Faella, E. Martinelli, E. Nigro, N. Salerno, M. Sabatino, G. Mantegazza: Aderenza tra calcestruzzo e fogli di FRP utilizzati come placcaggio di elementi inflessi. - Parte prima: risultati sperimentali, (in Italian) Proceedings of the XIV C.T.E. Conference, Mantua (Italy), november 2002;

(15) C. Faella, E. Martinelli, E. Nigro: Aderenza tra calcestruzzo e fogli di FRP utilizzati come placcaggio di elementi inflessi. - Parte seconda: modelli teorici ed elaborazioni numeriche, (in Italian) Proceedings of the XIV C.T.E. Conference, Mantua (Italy), november 2002.